AIMS Mathematics, 9(5): 11051–11075.
DOI: 10.3934/math.2024542
Received: 20 January 2024
Revised: 29 February 2024
Accepted: 04 March 2024
Published: 20 March 2024

http://www.aimspress.com/journal/Math

Research article

Exploration of nonlinear traveling wave phenomena in quintic conformable Benney-Lin equation within a liquid film

Noorah Mshary*

Department of Mathematics, Faculty of Science, Jazan University, P.O. Box 2097, Jazan 45142, Saudi Arabia

* **Correspondence:** Email: nmshary@jazanu.edu.sa.

Abstract: In this article, we use the modified extended direct algebraic method (mEDAM) to explore and analyze the traveling wave phenomena embedded in the quintic conformable Benney-Lin equation (CBLE) that regulates liquid film dynamics. The proposed transformation-based approach developed for nonlinear partial differential equations (PDEs) and fractional PDEs (FPDEs), efficiently produces a plethora of traveling wave solutions for the targeted CBLE, capturing the system's nuanced dynamics. The methodically determined traveling wave solutions are in the form of rational, exponential, hyperbolic and trigonometric functions which include periodic waves, bell-shaped kink waves and signal and double shock waves. To accurately depict the wave phenomena linked to these solutions, we generate 2D, 3D, and contour graphs. These visualizations not only improve understanding of the CBLE model's dynamics, but also provide a detailed way to examine its behavior. Moreover, the use of the proposed techniques contributes to a better understanding of the other FPDEs' distinct characteristics, enhancing our comprehension of their underpinning dynamics.

Keywords: fractional partial differential equations; fractional Benney-Lin equation; modified extended direct algebraic method; liquid film; traveling wave solutions; conformable derivatives
Mathematics Subject Classification: 33B15, 34A34, 35A20, 35A22, 44A10

1. Introduction

Using mathematical tools to solve real-world problems requires understanding of concepts such as rate of change, which is best achieved through the use of differential calculus. Regardless of its efficacy in estimating object speed over particular distances and times, numerous complex events which include singular formation, asymptotic characteristics, solitons, and chaos have frequently been overlooked or misunderstood. Calculus, which includes integral and differential operators, is essential for understanding real-world issues and predicting changes in natural phenomena. However, in the

realm of memory or genetic traits, investigators have discovered limitations in integer-order calculus, prompting mathematicians and physicists to develop fractional calculus (FC) with new operators. This has piqued the interest of academics investigating various FC models [1–3]. Academics have defined and explained FC and its foundational concepts, laying a solid foundation for this mathematical structure. FC has caught the interest of investigators exploring various ideas related to the rate of change as an extension of integer-order calculus. Scholars have used FC and its corresponding ramifications to elucidate resulting behaviors and are expecting applications in the future [4, 5].

The recent advancements in observer design methods for nonlinear generalized systems with nonlinear algebraic constraints, distributionally robust model predictive control with output feedback, and the computation of complex standard eigenvalue problem derivatives for laminar-turbulent transition prediction have significantly contributed to the field of control and automation [6]. In addition, iterative approximation techniques for fixed point problems and variational inequality problems on Hadamard manifolds have provided valuable insights into optimization and mathematical analysis [7]. These research endeavors have led to the development of innovative techniques and methodologies with broad applications across various domains, including robotics, aerospace engineering, and industrial automation [8]. This stage for exploring the latest developments in control theory and optimization strategies, showcasing the interdisciplinary nature and practical significance of these research endeavors [9].

Moreover, research on the behavior of nonlinear systems defined by differential equations has been sparked by recent developments in the discipline of FC. Nonlinear differential equations, which present analytical challenges in explaining various natural processes, have resulted in the development of several semi-analytical and iterative numerical methods. Mathematicians, engineers, and physicists have created new algorithms by leveraging advances in technology for computers and symbolic programming. Researchers can use these methodologies to present findings from simulations and analyze a wide range of nonlinear systems [10–14]. Notably, in [15, 16], authors investigated logistical models in the FC framework, yielding intriguing results. In [17], scientists investigated the most efficient methods for managing co-existing diabetes and tuberculosis using effective numerical methods; [18] also provided a thorough examination of general fractional derivatives and their possible uses, especially when understanding viscoelastic processes. These studies delve into topics like terahertz wavefront control using metasurfaces, fixed-time tracking control of nonlinear systems, reconfiguration strategies for formation flying, and the analysis of nonlinear wave equations [19, 20]. Each contribution adds a unique perspective to its respective field, offering insights into novel phenomena, theoretical frameworks, and practical applications [21, 22]. This compilation of research highlights the interdisciplinary nature of modern scientific inquiry and underscores the importance of collaboration and knowledge exchange across different domains [23–25].

Benney proposed the Benney-Lin Equation (BLE) [26] for analyzing the effects of long waves on liquid films in 1986, and Lin refined it later [27]. This paper focuses on the CBLE [28], incorporating the probability density function $v = v(x, t)$. The CBLE is a fractional generalization of the BLE, with conformable fractional derivatives replacing the temporal and spatial classical derivatives. The following is the mathematical illustration of this model:

$$D_t^{\mu} v + v D_x^{\lambda} v + D_{xxx}^{3\lambda} v + \beta(D_{xx}^{2\lambda} v + D_{xxxx}^{4\lambda} v) + \vartheta(D_{xxxxx}^{5\lambda} v) = 0. \tag{1.1}$$

By providing particular values to the pertinent real constants β and ϑ, Eq (1) is transformed into

the succinct Navier-Stokes equation in a solely dissipative form. This equation has been used to describe a variety of phenomena, including surface tension in liquid films, patterning of space in the Belousov-Zhabotinsky reaction, and erratic flame fronts. When certain conditions are satisfied, the equation translates into the fifth-order Korteweg-de Vries equation, referred to as the standard Kawahara equation, which provides insight into wave propagation with surface tension in its purely dispersive form (i.e., $\mu = \lambda = 1, \beta = 0$) [29]. Furthermore, the CBLE takes the form of the generalized Kuramoto-Sivashinsky equation when $\mu = \lambda = 1$ and $\vartheta = 0$. This dissipative-dispersive equation is used to explain waves in inclined and vertical falling films, uncertain drift waves in plasma, and tension between surfaces in liquid films caused by neighboring gas flow. In 1997, Biagioni and Linares [30] proved the universality of the CBLE's initial value problem in $H^s(R)$ for $s \geq 0$ when $\beta = 0$. Cui et al. [31] recently proved the local well-posedness of the Kawahara equation in the range $-1 < s < 1$ to 0 for $\beta = 0$. Furthermore, the CBLE has been studied using a variety of strategies, such as the residual power series method [32], the reduced differential transform method and the homotopy perturbation method [33], and the variational iteration method [34].

Researchers have developed a variety of analytical techniques to investigate traveling wave phenomena in nonlinear PDEs and FPDEs. The Bernoulli sub-equation method [35], Khater method [36], Kudryashov method [37], sine-Gordon method [38], exp-function method [39], $(\frac{G'}{G})$-expansion method [40], mEDAM method [41, 42], and many others [43–49] are notable examples. Among these techniques, the mEDAM has proven to be a dependable and efficient method for studying traveling wave phenomena in nonlinear FPDEs. By assuming a series-based solution, the FPDE is transformed into a nonlinear ordinary differential equation (NODE), which is then converted into a set of algebraic equations. In this investigation, the traveling wave, which is a self-sustaining disruption or oscillation that travels through a medium while maintaining its shape and speed over time, takes center stage. The primary goal is to investigate traveling wave phenomena in the CBLE via mEDAM by constructing traveling wave solutions for it [50–54].

2. Methodology materials

2.1. Conformable fractional derivative

It is feasible to arrive at explicit solutions for FPDEs by capitalizing on the advantages of conformable fractional derivatives over alternative fractional derivative operators. It is noteworthy that the traveling wave solutions of Eq (1.1) are impossible to deduce using alternative fractional derivative formulations due to chain rule violations [55, 56]. As a result, conformable fractional derivatives were added to Eq (1.1), [57] defines the conformable fractional derivative operator of order ν as:

$$D_\eta^\nu v(\eta) = \lim_{\gamma \to 0} \frac{v(\gamma \eta^{1-\nu} + \eta) - v(\eta)}{\gamma}, \quad \nu \in (0, 1]. \tag{2.1}$$

In this investigation, the following properties of this derivative are utilized:

$$D_\eta^\nu \eta^p = p\eta^{p-\nu}, \tag{2.2}$$

$$D_\eta^\nu (p_1 \rho(\eta) \pm p_2 \psi(\eta)) = p_1 D_\eta^\nu (\rho(\eta)) \pm p_2 D_\eta^\nu (\psi(\eta)), \tag{2.3}$$

$$D_\eta^\nu \chi[\zeta(\eta)] = \chi'_\zeta(\zeta(\eta)) D_\eta^\nu \zeta(\eta), \tag{2.4}$$

where $\rho(\eta)$, $\psi(\eta)$, $\chi(\eta)$ $\zeta(\eta)$ are arbitrary differentiable functions, whereas p, p_1, p_2 signify constants.

2.2. The working procedure of mEDAM

This section's goal is to present a general description of the mEDAM. Look into the FPDE in the following form:

$$E(v, D_t^{\alpha}v, D_{y_1}^{\beta}v, D_{y_2}^{\gamma}v, vD_{y_1}^{\beta}v, \ldots) = 0, \;\; 0 < \alpha, \beta, \gamma \leq 1, \tag{2.5}$$

where $v = v(t, y_1, y_2, y_3, \ldots, y_n)$. In order to solve Eq (2.5), the following steps are followed.

Step 1. Eq (2.5) is first subjected to a variable transformation of the form $v(t, y_1, y_2, y_3, ;y_n) = V(\eta)$, where η denotes a function of $t, y_1, y_2, y_3, ;y_n$ and may be expressed in a variety of ways. This transformation converts (2.5) into a NODE with its subsequent structure:

$$F(V, V', VV', \ldots) = 0. \tag{2.6}$$

The primes in (2.6) represent derivatives with regard to η. Equation (2.6) can occasionally be integrated once or more.

Step 2. Next, we suppose the subsequent closed form solution to (2.6):

$$V(\eta) = \sum_{l=0}^{N} q_j (B(\eta))^j. \tag{2.7}$$

Here, $q_j s$ symbolizes parameters which need to be estimated. Furthermore, $B(\eta)$ satisfies another NODE of the form:

$$B'(\eta) = d + eB(\eta) + f(B(\eta))^2, \tag{2.8}$$

where d, e, f are constants.

Step 3. We obtain a positive integer N (shown in Eq (2.7)) when we look for the homogeneous balance that exists between the prevailing nonlinear element and the greatest order derivative in Eq (2.6).

Step 4. We next put (2.7) into (2.6) or the equation obtained by integrating (2.6), and finally we put all the terms of $B(\eta)$ together in the same order, producing a polynomial in $B(\eta)$. A system of algebraic equations is produced for $q_j s$ and other parameters when the coefficients of the derived polynomial are all set to zero.

Step 5. Then, Maple is utilized to resolve this system of nonlinear algebraic equations.

Step 6. The traveling wave solutions to Eq (2.5) are found by determining the unknown parameters and plugging them into Eq (2.7) along with the associate solution $B(\eta)$ from Eq (2.8). Using the general solution of Eq (2.8), we can generate the families of traveling wave solutions shown below:

Family. 1: For $\varpi < 0$ and $f \neq 0$:

$$B_1(\eta) = -\frac{e}{2f} + \frac{\sqrt{-\varpi}\tan\left(\frac{1}{2}\sqrt{-\varpi}\eta\right)}{2f},$$

$$B_2(\eta) = -\frac{e}{2f} - \frac{\sqrt{-\varpi}\cot\left(\frac{1}{2}\sqrt{-\varpi}\eta\right)}{2f},$$

$$B_3(\eta) = -\frac{e}{2f} + \frac{\sqrt{-\varpi}\left(\tan\left(\sqrt{-\varpi}\eta\right) + \sec\left(\sqrt{-\varpi}\eta\right)\right)}{2f},$$

$$B_4(\eta) = -\frac{e}{2f} - \frac{\sqrt{-\varpi}\left(\cot\left(\sqrt{-\varpi}\eta\right) + \csc\left(\sqrt{-\varpi}\eta\right)\right)}{2f},$$

and

$$B_5(\eta) = -\frac{e}{2f} + \frac{\sqrt{-\varpi}\left(\tan\left(\frac{1}{4}\sqrt{-\varpi}\eta\right) - \cot\left(\frac{1}{4}\sqrt{-\varpi}\eta\right)\right)}{4f}.$$

Family. 2: For $\varpi > 0$ and $f \neq 0$:

$$B_6(\eta) = -\frac{e}{2f} - \frac{\sqrt{\varpi}\tanh\left(\frac{1}{2}\sqrt{\varpi}\eta\right)}{2f},$$

$$B_7(\eta) = -\frac{e}{2f} - \frac{\sqrt{\varpi}\coth\left(\frac{1}{2}\sqrt{\varpi}\eta\right)}{2f},$$

$$B_8(\eta) = -\frac{e}{2f} - \frac{\sqrt{\varpi}\left(\tanh\left(\sqrt{\varpi}\eta\right) + i\mathrm{sech}\left(\sqrt{\varpi}\eta\right)\right)}{2f},$$

$$B_9(\eta) = -\frac{e}{2f} - \frac{\sqrt{\varpi}\left(\coth\left(\sqrt{\varpi}\eta\right) + \mathrm{csch}\left(\sqrt{\varpi}\eta\right)\right)}{2f},$$

and

$$B_{10}(\eta) = -\frac{e}{2f} - \frac{\sqrt{\varpi}\left(\tanh\left(\frac{1}{4}\sqrt{\varpi}\eta\right) - \coth\left(\frac{1}{4}\sqrt{\varpi}\eta\right)\right)}{4f}.$$

Family. 3: For $df > 0$ and $e = 0$:

$$B_{11}(\eta) = \sqrt{\frac{d}{f}}\tan\left(\sqrt{df}\eta\right),$$

$$B_{12}(\eta) = -\sqrt{\frac{d}{f}}\cot\left(\sqrt{df}\eta\right),$$

$$B_{13}(\eta) = \sqrt{\frac{d}{f}}\left(\tan\left(2\sqrt{df}\eta\right) + \sec\left(2\sqrt{df}\eta\right)\right),$$

$$B_{14}(\eta) = -\sqrt{\frac{d}{f}}\left(\cot\left(2\sqrt{df}\eta\right) + \csc\left(2\sqrt{df}\eta\right)\right),$$

and

$$B_{15}(\eta) = \frac{1}{2}\sqrt{\frac{d}{f}}\left(\tan\left(\frac{1}{2}\sqrt{df}\eta\right) - \cot\left(\frac{1}{2}\sqrt{df}\eta\right)\right).$$

Family. 4: For $df < 0$ and $e = 0$:

$$B_{16}(\eta) = -\sqrt{-\frac{d}{f}}\tanh\left(\sqrt{-df}\eta\right),$$

$$B_{17}(\eta) = -\sqrt{-\frac{d}{f}}\coth\left(\sqrt{-df}\eta\right),$$

$$B_{18}(\eta) = -\sqrt{-\frac{d}{f}}\left(\tanh\left(2\sqrt{-df}\eta\right) + i\,\mathrm{sech}\left(2\sqrt{-df}\eta\right)\right),$$

$$B_{19}(\eta) = -\sqrt{-\frac{a}{c}}\left(\coth\left(2\sqrt{-df}\eta\right) + \mathrm{csch}\left(2\sqrt{-df}\eta\right)\right),$$

and

$$B_{20}(\eta) = -\frac{1}{2}\sqrt{-\frac{d}{f}}\left(\tanh\left(\frac{1}{2}\sqrt{-df}\eta\right) + \coth\left(\frac{1}{2}\sqrt{-df}\eta\right)\right).$$

Family. 5: For $f = d$ and $e = 0$:

$$B_{21}(\eta) = \tan(d\eta),$$

$$B_{22}(\eta) = -\cot(d\eta),$$

$$B_{23}(\eta) = \tan(2\,d\eta) + \sec(2\,d\eta),$$

$$B_{24}(\eta) = -\cot(2\,d\eta) + \csc(2\,d\eta),$$

and

$$B_{25}(\eta) = \frac{1}{2}\tan\left(\frac{1}{2}\,d\eta\right) - \frac{1}{2}\cot\left(\frac{1}{2}\,a\eta\right).$$

Family. 6: For $f = -d$ and $e = 0$:

$$B_{26}(\eta) = -\tanh(d\eta),$$

$$B_{27}(\eta) = -\coth(d\eta),$$

$$B_{28}(\eta) = -\tanh(2\,d\eta) + i\,\mathrm{sech}(2\,d\eta),$$

$$B_{29}(\eta) = -\coth(2\,d\eta) + \mathrm{csch}(2\,d\eta),$$

and

$$B_{30}(\eta) = -\frac{1}{2}\tanh\left(\frac{1}{2}\,d\eta\right) - \frac{1}{2}\coth\left(\frac{1}{2}\,d\eta\right).$$

Family. 7: For $\varpi = 0$:

$$B_{31}(\eta) = -2\,\frac{d\,(e\eta\,+2)}{e^2\eta}.$$

Family. 8: For $f = 0$, $e = \kappa$ and $d = s\kappa$ (with $s \neq 0$).

$$B_{32}(\eta) = \mathrm{e}^{\kappa\eta} - s.$$

Family. 9: For $e = f = 0$:

$$B_{33}(\eta) = d\eta.$$

Family. 10: For $e = d = 0$:

$$B_{34}(\eta) = -\frac{1}{f\eta}.$$

Family. 11: For $e \neq 0$, $f \neq 0$ and $d = 0$:

$$B_{35}(\eta) = -\frac{e}{f\left(\cosh\left(e\eta\right) - \sinh\left(e\eta\right) + 1\right)},$$

and

$$B_{36}(\eta) = -\frac{e\left(\cosh\left(e\eta\right) + \sinh\left(e\eta\right)\right)}{f\left(\cosh\left(e\eta\right) + \sinh\left(e\eta\right) + 1\right)}.$$

Family. 12: For $e = \kappa$, $f = s\kappa$ (with $s \neq 0$), and $d = 0$:

$$B_{37}(\eta) = \frac{\mathrm{e}^{\kappa\eta}}{1 - s\mathrm{e}^{\kappa\eta}}.$$

In the above solutions, $\varpi = e^2 - 4df$.

3. Traveling wave solutions

In this section we apply our suggested methods to the CBLE in (1.1) to generate traveling wave solutions for it. We begin with the transformation

$$v(x,t) = V(\eta); \quad \eta = \frac{x^{\lambda}}{\lambda} - \omega\frac{t^{\mu}}{\mu}, \tag{3.1}$$

which transforms (1.1) into the following NODE:

$$-\omega V' + VV' + V''' + \beta(V'' + V'''') + \vartheta V''''' = 0, \tag{3.2}$$

where V has derivatives with respect to η that are denoted by prime(s). Integrating (3.2) with respect to η and setting the constant of integration to zero yields:

$$-2\omega + V^2 + 2V'' + 2\beta(V' + V''') + 2\vartheta V'''' = 0. \tag{3.3}$$

Establishing the homogenous balance between V^2 V'''' in (3.3) gives $N + 4 = 2N$, which implies $N = 4$. Putting $N = 4$ in (2.7) gives the following solutions for (3.3):

$$V(\eta) = \sum_{l=0}^{4} q_l(B(\eta))^j = q_0 + q_1(B(\eta)) + q_2(B(\eta))^2 + q_3(B(\eta))^3 + q_4(B(\eta))^4. \tag{3.4}$$

To generate a system of algebraic equations, we substitute (3.4) in (3.3). Solving the resulting system using Maple, we get the following three cases of solutions:

Case. 1

$$\begin{aligned} &q_0 = \frac{1680}{13}\frac{f^2d^2}{\varpi}, q_1 = \frac{3360}{13}\frac{def^2}{\varpi}, q_2 = \frac{1680}{13}\frac{f^2\left(2fd + e^2\right)}{\varpi}, \\ &q_3 = \frac{3360}{13}\frac{ef^3}{\varpi}, q_4 = \frac{1680}{13}\frac{f^4}{\varpi}, \omega = \frac{36}{13}\varpi, \vartheta = -\frac{1}{13\varpi}, \beta = 0. \end{aligned} \tag{3.5}$$

Case. 2

$$q_0 = -12fd, q_1 = -12ef, q_2 = -12f^2, q_3 = 0, q_4 = 0, \omega = \varpi, \vartheta = 0, \beta = 0. \tag{3.6}$$

By taking into consideration case 1 and using (3.1), (3.4), and the corresponding general solution of (2.8), we construct the subsequent families of traveling wave solutions:
Family. 1.1: When $\varpi < 0, \quad f \neq 0$,

$$v_{1,1}(x,t) = \frac{105}{13}\,\frac{16\,f^2d^2 - 8\,de^2f + e^4 + 2\varpi^{\,2}\Big(\tan\Big(\frac{1}{2}\,\sqrt{-\varpi}\eta\Big)\Big)^2 + \varpi^2\Big(\tan\Big(\frac{1}{2}\,\sqrt{-\varpi}\eta\Big)\Big)^4}{\varpi}, \tag{3.7}$$

$$v_{1,2}(x,t) = \frac{105}{13}\,\frac{16\,f^2d^2 - 8\,de^2f + e^4 + 2\,e^2\varpi^{\,2}\Big(\cot\Big(\frac{1}{2}\,\sqrt{-\varpi}\eta\Big)\Big)^2 + \varpi^2\Big(\cot\Big(\frac{1}{2}\,\sqrt{-\varpi}\eta\Big)\Big)^4}{\varpi}, \tag{3.8}$$

$$\begin{aligned} v_{1,3}(x,t) &= \frac{1680}{13}\,\frac{f^2d^2}{\varpi} + \frac{3360def^2}{13\varpi}\Big(-\frac{1}{2}\,\frac{e}{f} + \frac{1}{2}\,\frac{\sqrt{-\varpi}\Big(\tan\Big(\sqrt{-\varpi}\eta\Big) + \sec\Big(\sqrt{-\varpi}\eta\Big)\Big)}{f}\Big) \\ &+ \frac{1680}{13\varpi}\,f^2\Big(2\,fd + e^2\Big)\Big(-\frac{1}{2}\,\frac{e}{f} + \frac{1}{2}\,\frac{\sqrt{-\varpi}\Big(\tan\Big(\sqrt{-\varpi}\eta\Big) + \sec\Big(\sqrt{-\varpi}\eta\Big)\Big)}{f}\Big)^2 \\ &+ \frac{3360}{13\varpi}\,ef^3\Big(-\frac{1}{2}\,\frac{e}{f} + \frac{1}{2}\,\frac{\sqrt{-\varpi}\Big(\tan\Big(\sqrt{-\varpi}\eta\Big) + \sec\Big(\sqrt{-\varpi}\eta\Big)\Big)}{f}\Big)^3 \\ &+ \frac{1680}{13\varpi}\,f^4\Big(-\frac{1}{2}\,\frac{e}{f} + \frac{1}{2}\,\frac{\sqrt{-\varpi}\Big(\tan\Big(\sqrt{-\varpi}\eta\Big) + \sec\Big(\sqrt{-\varpi}\eta\Big)\Big)}{f}\Big)^4, \end{aligned} \tag{3.9}$$

$$\begin{aligned} v_{1,4}(x,t) &= \frac{1680}{13}\,\frac{f^2d^2}{\varpi} + \frac{3360def^2}{13\varpi}\Big(-\frac{1}{2}\,\frac{e}{f} - \frac{1}{2}\,\frac{\sqrt{-\varpi}\Big(\cot\Big(\sqrt{-\varpi}\eta\Big) + \csc\Big(\sqrt{-\varpi}\eta\Big)\Big)}{f}\Big) \\ &+ \frac{1680}{13\varpi}\,f^2\Big(2\,fd + e^2\Big)\Big(-\frac{1}{2}\,\frac{e}{f} - \frac{1}{2}\,\frac{\sqrt{-\varpi}\Big(\cot\Big(\sqrt{-\varpi}\eta\Big) + \csc\Big(\sqrt{-\varpi}\eta\Big)\Big)}{f}\Big)^2 \\ &+ \frac{3360}{13\varpi}\,ef^3\Big(-\frac{1}{2}\,\frac{e}{f} - \frac{1}{2}\,\frac{\sqrt{-\varpi}\Big(\cot\Big(\sqrt{-\varpi}\eta\Big) + \csc\Big(\sqrt{-\varpi}\eta\Big)\Big)}{f}\Big)^3 \\ &+ \frac{1680}{13\varpi}\,f^4\Big(-\frac{1}{2}\,\frac{e}{f} - \frac{1}{2}\,\frac{\sqrt{-\varpi}\Big(\cot\Big(\sqrt{-\varpi}\eta\Big) + \csc\Big(\sqrt{-\varpi}\eta\Big)\Big)}{f}\Big)^4, \end{aligned} \tag{3.10}$$

and

$$
\begin{aligned}
v_{1,5}(x,t) &= \frac{1680}{13}\frac{f^2d^2}{\varpi} + \frac{3360def^2}{13\varpi}\Big(-\frac{1}{2}\frac{e}{f} + \frac{1}{4}\frac{\sqrt{-\varpi}\Big(\tan\Big(\frac{1}{4}\sqrt{-\varpi}\eta\Big) - \cot\Big(1/4\sqrt{-\varpi}\eta\Big)\Big)}{f}\Big)\\
&+ \frac{1680}{13\varpi}f^2\Big(2fd+e^2\Big)\Big(-\frac{1}{2}\frac{e}{f} + \frac{1}{4}\frac{\sqrt{-\varpi}\Big(\tan\Big(\frac{1}{4}\sqrt{-\varpi}\eta\Big) - \cot\Big(\frac{1}{4}\sqrt{-\varpi}\eta\Big)\Big)}{f}\Big)^2\\
&+ \frac{3360}{13\varpi}ef^3\Big(-\frac{1}{2}\frac{e}{f} + \frac{1}{4}\frac{\sqrt{-\varpi}\Big(\tan\Big(\frac{1}{4}\sqrt{-\varpi}\eta\Big) - \cot\Big(\frac{1}{4}\sqrt{-\varpi}\eta\Big)\Big)}{f}\Big)^3\\
&+ \frac{1680}{13\varpi}f^4\Big(-\frac{1}{2}\frac{e}{f} + \frac{1}{4}\frac{\sqrt{-\varpi}\Big(\tan\Big(\frac{1}{4}\sqrt{-\varpi}\eta\Big) - \cot\Big(\frac{1}{4}\sqrt{-\varpi}\eta\Big)\Big)}{f}\Big)^4.
\end{aligned}
\tag{3.11}
$$

Family. 1.2: When $\varpi > 0, \quad f \neq 0,$

$$
v_{1,6}(x,t) = \frac{105}{13}\frac{16f^2d^2 - 8de^2f + e^4 - 2e^2\varpi^2\Big(\tanh\Big(\frac{1}{2}\sqrt{\varpi}\eta\Big)\Big)^2 + \varpi^2\Big(\tanh\Big(\frac{1}{2}\sqrt{\varpi}\eta\Big)\Big)^4}{\varpi},
\tag{3.12}
$$

$$
v_{1,7}(x,t) = \frac{105}{13}\frac{16f^2d^2 - 8de^2f + e^4 - 2e^2\varpi^2\Big(\coth\Big(\frac{1}{2}\sqrt{\varpi}\eta\Big)\Big)^2 + \varpi^2\Big(\coth\Big(\frac{1}{2}\sqrt{\varpi}\eta\Big)\Big)^4}{\varpi},
\tag{3.13}
$$

$$
\begin{aligned}
v_{1,8}(x,t) &= \frac{1680}{13}\frac{f^2d^2}{\varpi} + \frac{3360def^2}{13\varpi}\Big(-\frac{1}{2}\frac{e}{f} - \frac{1}{2}\frac{\sqrt{\varpi}\Big(\tanh\Big(\sqrt{\varpi}\eta\Big) + i\mathrm{sech}\Big(\sqrt{\varpi}\eta\Big)\Big)}{f}\Big)\\
&+ \frac{1680}{13\varpi}f^2\Big(2fd+e^2\Big)\Big(-\frac{1}{2}\frac{e}{f} - \frac{1}{2}\frac{\sqrt{\varpi}\Big(\tanh\Big(\sqrt{\varpi}\eta\Big) + i\mathrm{sech}\Big(\sqrt{\varpi}\eta\Big)\Big)}{f}\Big)^2\\
&+ \frac{3360}{13\varpi}ef^3\Big(-\frac{1}{2}\frac{e}{f} - \frac{1}{2}\frac{\sqrt{\varpi}\Big(\tanh\Big(\sqrt{\varpi}\eta\Big) + i\mathrm{sech}\Big(\sqrt{\varpi}\eta\Big)\Big)}{f}\Big)^3\\
&+ \frac{1680}{13\varpi}f^4\Big(-\frac{1}{2}\frac{e}{f} - \frac{1}{2}\frac{\sqrt{\varpi}\Big(\tanh\Big(\sqrt{\varpi}\eta\Big) + i\mathrm{sech}\Big(\sqrt{\varpi}\eta\Big)\Big)}{f}\Big)^4,
\end{aligned}
\tag{3.14}
$$

$$
\begin{aligned}
v_{1,9}(x,t) &= \frac{1680}{13}\frac{f^2d^2}{\varpi} + \frac{3360def^2}{13\varpi}\Big(-\frac{1}{2}\frac{e}{f} - \frac{1}{2}\frac{\sqrt{\varpi}\Big(\coth\Big(\sqrt{\varpi}\eta\Big) + \operatorname{csch}\Big(\sqrt{\varpi}\eta\Big)\Big)}{f}\Big) \\
&+ \frac{1680}{13\varpi}f^2\Big(2fd+e^2\Big)\Big(-\frac{1}{2}\frac{e}{f} - \frac{1}{2}\frac{\sqrt{\varpi}\Big(\coth\Big(\sqrt{\varpi}\eta\Big) + \operatorname{csch}\Big(\sqrt{\varpi}\eta\Big)\Big)}{f}\Big)^2 \\
&+ \frac{3360}{13\varpi}ef^3\Big(-\frac{1}{2}\frac{e}{f} - \frac{1}{2}\frac{\sqrt{\varpi}\Big(\coth\Big(\sqrt{\varpi}\eta\Big) + \operatorname{csch}\Big(\sqrt{\varpi}\eta\Big)\Big)}{f}\Big)^3 \\
&+ \frac{1680}{13\varpi}f^4\Big(-\frac{1}{2}\frac{e}{f} - \frac{1}{2}\frac{\sqrt{\varpi}\Big(\coth\Big(\sqrt{\varpi}\eta\Big) + \operatorname{csch}\Big(\sqrt{\varpi}\eta\Big)\Big)}{f}\Big)^4,
\end{aligned}
\tag{3.15}
$$

and

$$
\begin{aligned}
v_{1,10}(x,t) &= \frac{1680}{13}\frac{f^2d^2}{\varpi} + \frac{3360def^2}{13\varpi}\Big(-\frac{1}{2}\frac{e}{f} - \frac{1}{4}\frac{\sqrt{\varpi}\Big(\tanh\Big(\frac{1}{4}\sqrt{\varpi}\eta\Big) - \coth\Big(1/4\sqrt{\varpi}\eta\Big)\Big)}{f}\Big) \\
&+ \frac{1680}{13\varpi}f^2\Big(2fd+e^2\Big)\Big(-\frac{1}{2}\frac{e}{f} - \frac{1}{4}\frac{\sqrt{\varpi}\Big(\tanh\Big(\frac{1}{4}\sqrt{\varpi}\eta\Big) - \coth\Big(1/4\sqrt{\varpi}\eta\Big)\Big)}{f}\Big)^2 \\
&+ \frac{3360}{13\varpi}ef^3\Big(-\frac{1}{2}\frac{e}{f} - \frac{1}{4}\frac{\sqrt{\varpi}\Big(\tanh\Big(\frac{1}{4}\sqrt{\varpi}\eta\Big) - \coth\Big(\frac{1}{4}\sqrt{\varpi}\eta\Big)\Big)}{f}\Big)^3 \\
&+ \frac{1680}{13\varpi}f^4\Big(-\frac{1}{2}\frac{e}{f} - \frac{1}{4}\frac{\sqrt{\varpi}\Big(\tanh\Big(\frac{1}{4}\sqrt{\varpi}\eta\Big) - \coth\Big(\frac{1}{4}\sqrt{\varpi}\eta\Big)\Big)}{f}\Big)^4.
\end{aligned}
\tag{3.16}
$$

Family. 1.3: When $df > 0$ and $e = 0$,

$$
v_{1,11}(x,t) = \frac{1680}{13}\frac{f^2d^2}{\varpi} + \frac{3360}{13}\frac{f^2d^2\Big(\tan\Big(\sqrt{fd}\eta\Big)\Big)^2}{\varpi} + \frac{1680}{13}\frac{f^2d^2\Big(\tan\Big(\sqrt{fd}\eta\Big)\Big)^4}{\varpi},
\tag{3.17}
$$

$$
v_{1,12}(x,t) = \frac{1680}{13}\frac{f^2d^2}{\varpi} + \frac{3360}{13}\frac{f^2d^2\Big(\cot\Big(\sqrt{fd}\eta\Big)\Big)^2}{\varpi} + \frac{1680}{13}\frac{f^2d^2\Big(\cot\Big(\sqrt{fd}\eta\Big)\Big)^4}{\varpi},
\tag{3.18}
$$

$$
\begin{aligned}
v_{1,13}(x,t) &= \frac{3360}{13}\frac{f^2d^2\Big(\tan\Big(2\sqrt{fd}\eta\Big) + \sec\Big(2\sqrt{fd}\eta\Big)\Big)^2}{\varpi} \\
&+ \frac{1680}{13}\frac{f^2d^2\Big(\tan\Big(2\sqrt{fd}\eta\Big) + \sec\Big(2\sqrt{fd}\eta\Big)\Big)^4}{\varpi} + \frac{1680}{13}\frac{f^2d^2}{\varpi},
\end{aligned}
\tag{3.19}
$$

$$v_{1,14}(x,t) = \frac{3360}{13}\frac{f^2d^2\left(\cot\left(2\sqrt{fd}\eta\right)+\csc\left(2\sqrt{fd}\eta\right)\right)^2}{\varpi} + \frac{1680}{13}\frac{f^2d^2\left(\cot\left(2\sqrt{fd}\eta\right)+\csc\left(2\sqrt{fd}\eta\right)\right)^4}{\varpi} + \frac{1680}{13}\frac{f^2d^2}{\varpi}, \tag{3.20}$$

and

$$v_{1,15}(x,t) = \frac{840}{13}\frac{f^2d^2\left(\tan\left(\frac{1}{2}\sqrt{fd}\eta\right)-\cot\left(\frac{1}{2}\sqrt{fd}\eta\right)\right)^2}{\varpi} + \frac{105}{13}\frac{f^2d^2\left(\tan\left(\frac{1}{2}\sqrt{fd}\eta\right)-\cot\left(\frac{1}{2}\sqrt{fd}\eta\right)\right)^4}{\varpi} + \frac{1680}{13}\frac{f^2d^2}{\varpi}. \tag{3.21}$$

Family. 1.4: When $df < 0$ and $e = 0$,

$$v_{1,16}(x,t) = \frac{1680}{13}\frac{f^2d^2}{\varpi} - \frac{3360}{13}\frac{f^2d^2\left(\tanh\left(\sqrt{-fd}\eta\right)\right)^2}{\varpi} + \frac{1680}{13}\frac{f^2d^2\left(\tanh\left(\sqrt{-fd}\eta\right)\right)^4}{\varpi}, \tag{3.22}$$

$$v_{1,17}(x,t) = \frac{1680}{13}\frac{f^2d^2}{\varpi} - \frac{3360}{13}\frac{f^2d^2\left(\coth\left(\sqrt{-fd}\eta\right)\right)^2}{\varpi} + \frac{1680}{13}\frac{f^2d^2\left(\coth\left(\sqrt{-fd}\eta\right)\right)^4}{\varpi}, \tag{3.23}$$

$$v_{1,18}(x,t) = -\frac{3360}{13}\frac{f^2d^2\left(\tanh\left(2\sqrt{-fd}\eta\right)+i\mathrm{sech}\left(2\sqrt{-fd}\eta\right)\right)^2}{\varpi} + \frac{1680}{13}\frac{f^2d^2\left(\tanh\left(2\sqrt{-fd}\eta\right)+i\mathrm{sech}\left(2\sqrt{-fd}\eta\right)\right)^4}{\varpi} + \frac{1680}{13}\frac{f^2d^2}{\varpi}, \tag{3.24}$$

$$v_{1,19}(x,t) = -\frac{3360}{13}\frac{f^2d^2\left(\coth\left(2\sqrt{-fd}\eta\right)+\mathrm{csch}\left(2\sqrt{-fd}\eta\right)\right)^2}{\varpi} + \frac{1680}{13}\frac{f^2d^2\left(\coth\left(2\sqrt{-fd}\eta\right)+\mathrm{csch}\left(2\sqrt{-fd}\eta\right)\right)^4}{\varpi} + \frac{1680}{13}\frac{f^2d^2}{\varpi}, \tag{3.25}$$

and

$$v_{1,20}(x,t) = -\frac{840}{13}\frac{f^2d^2\left(\tanh\left(\frac{1}{2}\sqrt{-fd}\eta\right)+\coth\left(\frac{1}{2}\sqrt{-fd}\eta\right)\right)^2}{\varpi} + \frac{105}{13}\frac{f^2d^2\left(\tanh\left(\frac{1}{2}\sqrt{-fd}\eta\right)+\coth\left(\frac{1}{2}\sqrt{-fd}\eta\right)\right)^4}{\varpi} + \frac{1680}{13}\frac{f^2d^2}{\varpi}. \tag{3.26}$$

Family. 1.5: When $f = d$ and $e = 0$,

$$v_{1,21}(x,t) = \frac{1680}{13}\frac{d^4}{\varpi} + \frac{3360}{13}\frac{d^4\Big(\tan\Big(d\eta\Big)\Big)^2}{\varpi} + \frac{1680}{13}\frac{d^4\Big(\tan\Big(d\eta\Big)\Big)^4}{\varpi}, \tag{3.27}$$

$$v_{1,22}(x,t) = \frac{1680}{13}\frac{d^4}{\varpi} + \frac{3360}{13}\frac{d^4\Big(\cot\Big(d\eta\Big)\Big)^2}{\varpi} + \frac{1680}{13}\frac{d^4\Big(\cot\Big(d\eta\Big)\Big)^4}{\varpi}, \tag{3.28}$$

$$\begin{aligned} v_{1,23}(x,t) = {} & \frac{3360}{13}\frac{d^4\Big(\tan\Big(2\,d\eta\Big) + \sec\Big(2\,d\eta\Big)\Big)^2}{\varpi} \\ & + \frac{1680}{13}\frac{d^4\Big(\tan\Big(2\,d\eta\Big) + \sec\Big(2\,d\eta\Big)\Big)^4}{\varpi} + \frac{1680}{13}\frac{d^4}{\varpi}, \end{aligned} \tag{3.29}$$

$$\begin{aligned} v_{1,24}(x,t) = {} & \frac{3360}{13}\frac{d^4\Big(-\cot\Big(2\,d\eta\Big) - \csc\Big(2\,d\eta\Big)\Big)^2}{\varpi} \\ & + \frac{1680}{13}\frac{d^4\Big(-\cot\Big(2\,d\eta\Big) - \csc\Big(2\,d\eta\Big)\Big)^4}{\varpi} + \frac{1680}{13}\frac{d^4}{\varpi}, \end{aligned} \tag{3.30}$$

and

$$\begin{aligned} v_{1,25}(x,t) = {} & \frac{3360}{13}\frac{d^4\Big(\frac{1}{2}\tan\Big(\frac{1}{2}\,d\eta\Big) - \frac{1}{2}\cot\Big(\frac{1}{2}\,d\eta\Big)\Big)^2}{\varpi} \\ & + \frac{1680}{13}\frac{d^4\Big(\frac{1}{2}\tan\Big(\frac{1}{2}\,d\eta\Big) - \frac{1}{2}\cot\Big(\frac{1}{2}\,d\eta\Big)\Big)^4}{\varpi} + \frac{1680}{13}\frac{d^4}{\varpi}. \end{aligned} \tag{3.31}$$

Family. 1.6: When $f = -d$ and $e = 0$,

$$v_{1,26}(x,t) = \frac{1680}{13}\frac{d^4}{\varpi} - \frac{3360}{13}\frac{d^4\Big(\tanh\Big(d\eta\Big)\Big)^2}{\varpi} + \frac{1680}{13}\frac{d^4\Big(\tanh\Big(d\eta\Big)\Big)^4}{\varpi}, \tag{3.32}$$

$$v_{1,27}(x,t) = \frac{1680}{13}\frac{d^4}{\varpi} - \frac{3360}{13}\frac{d^4\Big(\coth\Big(d\eta\Big)\Big)^2}{\varpi} + \frac{1680}{13}\frac{d^4\Big(\coth\Big(d\eta\Big)\Big)^4}{\varpi}, \tag{3.33}$$

$$\begin{aligned} v_{1,28}(x,t) = {} & -\frac{3360}{13}\frac{d^4\Big(-\tanh\Big(2\,d\eta\Big) - i\mathrm{sech}\Big(2\,d\eta\Big)\Big)^2}{\varpi} \\ & + \frac{1680}{13}\frac{d^4\Big(-\tanh\Big(2\,d\eta\Big) - i\mathrm{sech}\Big(2\,d\eta\Big)\Big)^4}{\varpi} + \frac{1680}{13}\frac{d^4}{\varpi}, \end{aligned} \tag{3.34}$$

$$v_{1,29}(x,t) = -\frac{3360}{13}\frac{d^4\Big(-\coth\Big(2\,d\eta\Big)-\operatorname{csch}\Big(2\,d\eta\Big)\Big)^2}{\varpi} + \frac{1680}{13}\frac{d^4\Big(-\coth\Big(2\,d\eta\Big)-\operatorname{csch}\Big(2\,d\eta\Big)\Big)^4}{\varpi} + \frac{1680}{13}\frac{d^4}{\varpi}, \tag{3.35}$$

and

$$v_{1,30}(x,t) = -\frac{3360}{13}\frac{d^4\Big(-\frac{1}{2}\tanh\Big(\frac{1}{2}\,d\eta\Big)-\frac{1}{2}\coth\Big(\frac{1}{2}\,d\eta\Big)\Big)^2}{\varpi} + \frac{1680}{13}\frac{d^4\Big(-\frac{1}{2}\tanh\Big(\frac{1}{2}\,d\eta\Big)-1/2\coth\Big(\frac{1}{2}\,d\eta\Big)\Big)^4}{\varpi} + \frac{1680}{13}\frac{d^4}{\varpi}. \tag{3.36}$$

Family. 1.7: When $d = 0$, $e \neq 0$, and $e \neq 0$,

$$v_{1,31}(x,t) = \frac{1680}{13}\frac{e^4\Big(2\Big(\cosh\Big(e\eta\Big)\Big)^2-2\cosh\Big(e\eta\Big)\sinh\Big(e\eta\Big)-1\Big)}{\varpi\Big(\cosh\Big(e\eta\Big)-\sinh\Big(e\eta\Big)+1\Big)^4}, \tag{3.37}$$

and

$$v_{1,32}(x,t) = \frac{1680}{13}\frac{e^4\Big(\cosh\Big(e\eta\Big)+\sinh\Big(e\eta\Big)\Big)^2}{\varpi\Big(\cosh\Big(e\eta\Big)+\sinh\Big(e\eta\Big)+1\Big)^4}. \tag{3.38}$$

Family. 1.8: When $e = \kappa$, $f = s\kappa(s \neq 0)$, and $d = 0$,

$$v_{1,33}(x,t) = \frac{1680}{13}\frac{s^2\kappa^4 \mathrm{e}^{2\kappa\eta}p^2}{\varpi\Big(-p+s\mathrm{e}^{\kappa\eta}\Big)^4}. \tag{3.39}$$

$\eta = \frac{x^\lambda}{\lambda} - (\frac{36}{13}\,\varpi)\frac{t^\mu}{\mu}$.

By taking into consideration case 2 and using (3.1), (3.4), and the corresponding general solution of (2.8), we construct the subsequent families of traveling wave solutions:

Family. 2.1: When $\varpi < 0, \quad f \neq 0$,

$$v_{2,1}(x,t) = -12\,ef\Big(-\frac{1}{2}\frac{e}{f}+\frac{1}{2}\frac{\sqrt{-\varpi}\tan\Big(\frac{1}{2}\sqrt{-\varpi}\eta\Big)}{f}\Big) - 12\,f^2\Big(-\frac{1}{2}\frac{e}{f}+\frac{1}{2}\frac{\sqrt{-\varpi}\tan\Big(\frac{1}{2}\sqrt{-\varpi}\eta\Big)}{f}\Big)^2 - 12\,fd, \tag{3.40}$$

$$v_{2,2}(x,t) = -12\,ef\Big(-\frac{1}{2}\frac{e}{f} - \frac{1}{2}\frac{\sqrt{-\varpi}\cot\left(\frac{1}{2}\sqrt{-\varpi}\eta\right)}{f}\Big) - 12\,f^2\Big(-\frac{1}{2}\frac{e}{f} - \frac{1}{2}\frac{\sqrt{-\varpi}\cot\left(\frac{1}{2}\sqrt{-\varpi}\eta\right)}{f}\Big)^2 - 12\,fd, \tag{3.41}$$

$$v_{2,3}(x,t) = -12\,ef\Big(-\frac{1}{2}\frac{e}{f} + \frac{1}{2}\frac{\sqrt{-\varpi}\Big(\tan\left(\sqrt{-\varpi}\eta\right) + \sec\left(\sqrt{-\varpi}\eta\right)\Big)}{f}\Big) - 12\,f^2\Big(-\frac{1}{2}\frac{e}{f} + \frac{1}{2}\frac{\sqrt{-\varpi}\Big(\tan\left(\sqrt{-\varpi}\eta\right) + \sec\left(\sqrt{-\varpi}\eta\right)\Big)}{f}\Big)^2 - 12\,fd, \tag{3.42}$$

$$v_{2,4}(x,t) = -12\,ef\Big(-\frac{1}{2}\frac{e}{f} - \frac{1}{2}\frac{\sqrt{-\varpi}\Big(\cot\left(\sqrt{-\varpi}\eta\right) + \csc\left(\sqrt{-\varpi}\eta\right)\Big)}{f}\Big) - 12\,f^2\Big(-\frac{1}{2}\frac{e}{f} - \frac{1}{2}\frac{\sqrt{-\varpi}\Big(\cot\left(\sqrt{-\varpi}\eta\right) + \csc\left(\sqrt{-\varpi}\eta\right)\Big)}{f}\Big)^2 - 12\,fd, \tag{3.43}$$

and

$$v_{2,5}(x,t) = -12\,ef\Big(-\frac{1}{2}\frac{e}{f} + \frac{1}{4}\frac{\sqrt{-\varpi}\Big(\tan\left(\frac{1}{4}\sqrt{-\varpi}\eta\right) - \cot\left(\frac{1}{4}\sqrt{-\varpi}\eta\right)\Big)}{f}\Big) - 12\,f^2\Big(-\frac{1}{2}\frac{e}{f} + \frac{1}{4}\frac{\sqrt{-\varpi}\Big(\tan\left(\frac{1}{4}\sqrt{-\varpi}\eta\right) - \cot\left(\frac{1}{4}\sqrt{-\varpi}\eta\right)\Big)}{f}\Big)^2 - 12\,fd. \tag{3.44}$$

Family. 2.2: When $\varpi > 0, \quad f \neq 0,$

$$v_{2,6}(x,t) = -12\,ef\Big(-\frac{1}{2}\frac{e}{f} - \frac{1}{2}\frac{\sqrt{\varpi}\tanh\left(\frac{1}{2}\sqrt{\varpi}\eta\right)}{f}\Big) - 12\,f^2\Big(-\frac{1}{2}\frac{e}{f} - \frac{1}{2}\frac{\sqrt{\varpi}\tanh\left(\frac{1}{2}\sqrt{\varpi}\eta\right)}{f}\Big)^2 - 12\,fd, \tag{3.45}$$

$$v_{2,7}(x,t) = -12\,ef\Big(-\frac{1}{2}\frac{e}{f} - \frac{1}{2}\frac{\sqrt{\varpi}\coth\left(\frac{1}{2}\sqrt{\varpi}\eta\right)}{f}\Big) - 12\,f^2\Big(-\frac{1}{2}\frac{e}{f} - \frac{1}{2}\frac{\sqrt{\varpi}\coth\left(\frac{1}{2}\sqrt{\varpi}\eta\right)}{f}\Big)^2 - 12\,fd, \tag{3.46}$$

$$v_{2,8}(x,t) = -12\,ef\Big(-\frac{1}{2}\frac{e}{f} - \frac{1}{2}\frac{\sqrt{\varpi}\Big(\tanh\Big(\sqrt{\varpi}\eta\Big) + i\mathrm{sech}\Big(\sqrt{\varpi}\eta\Big)\Big)}{f}\Big)$$
$$-12\,f^2\Big(-\frac{1}{2}\frac{e}{f} - \frac{1}{2}\frac{\sqrt{\varpi}\Big(\tanh\Big(\sqrt{\varpi}\eta\Big) + i\mathrm{sech}\Big(\sqrt{\varpi}\eta\Big)\Big)}{f}\Big)^2 - 12\,fd, \tag{3.47}$$

$$v_{2,9}(x,t) = -12\,ef\Big(-\frac{1}{2}\frac{e}{f} - \frac{1}{2}\frac{\sqrt{\varpi}\Big(\coth\Big(\sqrt{\varpi}\eta\Big) + \mathrm{csch}\Big(\sqrt{\varpi}\eta\Big)\Big)}{f}\Big)$$
$$-12\,f^2\Big(-\frac{1}{2}\frac{e}{f} - \frac{1}{2}\frac{\sqrt{\varpi}\Big(\coth\Big(\sqrt{\varpi}\eta\Big) + \mathrm{csch}\Big(\sqrt{\varpi}\eta\Big)\Big)}{f}\Big)^2 - 12\,fd, \tag{3.48}$$

and

$$v_{2,10}(x,t) = -12\,ef\Big(-\frac{1}{2}\frac{e}{f} - \frac{1}{4}\frac{\sqrt{\varpi}\Big(\tanh\Big(\frac{1}{4}\sqrt{\varpi}\eta\Big) - \coth\Big(\frac{1}{4}\sqrt{\varpi}\eta\Big)\Big)}{f}\Big)$$
$$-12\,f^2\Big(-\frac{1}{2}\frac{e}{f} - \frac{1}{4}\frac{\sqrt{\varpi}\Big(\tanh\Big(\frac{1}{4}\sqrt{\varpi}\eta\Big) - \coth\Big(\frac{1}{4}\sqrt{\varpi}\eta\Big)\Big)}{f}\Big)^2 - 12\,fd. \tag{3.49}$$

Family. 2.3: When $df > 0$ and $e = 0$,

$$v_{2,11}(x,t) = -12\,fd - 12\,fd\Big(\tan\Big(\sqrt{fd}\eta\Big)\Big)^2, \tag{3.50}$$

$$v_{2,12}(x,t) = -12\,fd - 12\,fd\Big(\cot\Big(\sqrt{fd}\eta\Big)\Big)^2, \tag{3.51}$$

$$v_{2,13}(x,t) = -12\,fd - 12\,fd\Big(\tan\Big(2\,\sqrt{fd}\eta\Big) + \sec\Big(2\,\sqrt{fd}\eta\Big)\Big)^2, \tag{3.52}$$

$$v_{2,14}(x,t) = -12\,fd - 12\,fd\Big(\cot\Big(2\,\sqrt{fd}\eta\Big) + \csc\Big(2\,\sqrt{fd}\eta\Big)\Big)^2, \tag{3.53}$$

and

$$v_{2,15}(x,t) = -12\,fd - 3\,fd\Big(\tan\Big(\frac{1}{2}\,\sqrt{fd}\eta\Big) - \cot\Big(\frac{1}{2}\,\sqrt{fd}\eta\Big)\Big)^2. \tag{3.54}$$

Family. 2.4: When $df < 0$ and $e = 0$,

$$v_{2,16}(x,t) = -12\,fd + 12\,fd\Big(\tanh\Big(\sqrt{-fd}\eta\Big)\Big)^2, \tag{3.55}$$

$$v_{2,17}(x,t) = -12\,fd + 12\,fd\Big(\coth\Big(\sqrt{-fd}\eta\Big)\Big)^2, \tag{3.56}$$

$$v_{2,18}(x,t) = -12\,fd + 12\,fd\Big(\tanh\Big(2\,\sqrt{-fd}\eta\Big) + i\mathrm{sech}\Big(2\,\sqrt{-fd}\eta\Big)\Big)^2, \tag{3.57}$$

$$v_{2,19}(x,t) = -12\,fd + 12\,fd\Big(\coth\Big(2\,\sqrt{-fd}\eta\Big) + \mathrm{csch}\Big(2\,\sqrt{-fd}\eta\Big)\Big)^2, \tag{3.58}$$

and

$$v_{2,20}(x,t) = -12\,fd + 3\,fd\Big(\tanh\Big(\frac{1}{2}\,\sqrt{-fd}\eta\Big) + \coth\Big(\frac{1}{2}\,\sqrt{-fd}\eta\Big)\Big)^2. \tag{3.59}$$

Family. 2.5: When $f = d$ and $e = 0$,

$$v_{2,21}(x,t) = -12\,d^2 - 12\,d^2\Big(\tan\Big(d\eta\Big)\Big)^2, \tag{3.60}$$

$$v_{2,22}(x,t) = -12\,d^2 - 12\,d^2\Big(\cot\Big(d\eta\Big)\Big)^2, \tag{3.61}$$

$$v_{2,23}(x,t) = -12\,d^2 - 12\,d^2\Big(\tan\Big(2\,d\eta\Big) + \sec\Big(2\,d\eta\Big)\Big)^2, \tag{3.62}$$

$$v_{2,24}(x,t) = -12\,d^2 - 12\,d^2\Big(-\cot\Big(2\,d\eta\Big) - \csc\Big(2\,d\eta\Big)\Big)^2, \tag{3.63}$$

and

$$v_{2,25}(x,t) = -12\,d^2 - 12\,d^2\Big(\frac{1}{2}\,\tan\Big(\frac{1}{2}\,d\eta\Big) - \frac{1}{2}\cot\Big(\frac{1}{2}\,d\eta\Big)\Big)^2. \tag{3.64}$$

Family. 2.6: When $f = -d$ and $e = 0$,

$$v_{2,26}(x,t) = 12\,d^2 - 12\,d^2\Big(\tanh\Big(d\eta\Big)\Big)^2, \tag{3.65}$$

$$v_{2,27}(x,t) = 12\,d^2 - 12\,d^2\Big(\coth\Big(d\eta\Big)\Big)^2, \tag{3.66}$$

$$v_{2,28}(x,t) = 12\,d^2 - 12\,d^2\Big(-\tanh\Big(2\,d\eta\Big) - i\mathrm{sech}\Big(2\,d\eta\Big)\Big)^2, \tag{3.67}$$

$$v_{2,29}(x,t) = 12\,d^2 - 12\,d^2\Big(-\coth\Big(2\,d\eta\Big) - \mathrm{csch}\Big(2\,d\eta\Big)\Big)^2, \tag{3.68}$$

and

$$v_{2,30}(x,t) = 12\,d^2 - 12\,d^2\Big(-\frac{1}{2}\,\tanh\Big(\frac{1}{2}\,d\eta\Big) - \frac{1}{2}\,\coth\Big(\frac{1}{2}\,d\eta\Big)\Big)^2. \tag{3.69}$$

Family. 2.7: When $\varpi = 0$,

$$v_{2,31}(x,t) = -12\,df + 24\,\frac{fd\Big(e\eta + 2\Big)}{e\eta} - 48\,\frac{f^2\Big(d\Big(e\eta + 2\Big)\Big)^2}{e^4\eta^2}. \tag{3.70}$$

Family. 2.8: When $e = d = 0$,

$$v_{2,32}(x,t) = -12\,\eta^{-2}. \tag{3.71}$$

Family. 2.9: When $d = 0$, $e \neq 0$, and $e \neq 0$,

$$v_{2,33}(x,t) = 12\,\frac{e^2\Big(\cosh\Big(e\eta\Big) - \sinh\Big(e\eta\Big)\Big)}{\Big(\cosh\Big(e\eta\Big) - \sinh\Big(e\eta\Big) + 1\Big)^2}, \tag{3.72}$$

and

$$v_{2,34}(x,t) = 12\,\frac{e^2\Big(\cosh\Big(e\eta\Big) + \sinh\Big(e\eta\Big)\Big)}{\Big(\cosh\Big(e\eta\Big) + \sinh\Big(e\eta\Big) + 1\Big)^2}. \tag{3.73}$$

Family. 2.10: When $e = \kappa$, $f = s\kappa(s \neq 0)$, and $d = 0$,

$$v_{2,35}(x,t) = -12\,\frac{\kappa^2 s\mathrm{e}^{\kappa\eta}}{\Big(-1 + s\mathrm{e}^{\kappa\eta}\Big)^2}. \tag{3.74}$$

$\eta = \frac{x^\lambda}{\lambda} - \varpi\frac{t^\mu}{\mu}$.

4. Discussion and graphs

The various wave patterns found in the examined models are displayed in this section. The used fractional derivative operator, i.e., conformable derivative, and the proposed mEDAM allowed us to extract and render these wave structures in three different formats: two dimensions, three dimensions, and contour representations. These depictions comprise bell-shaped, periodic, kink, and shock propagating wave solutions. Precise choices of parameters produce displays that are both aesthetically pleasing and instructive. Interestingly, the study's results are distinct; to the greatest extent of our knowing, this technique's findings have never been used in the published literature to address CBLE.

Shock waves are fast, high-energy interruptions that signal abrupt, significant shifts in a medium's temperature, pressure, and density. They are commonly associated with supersonic flows. Kink waves, which are characterized by compression or twisting as they travel across a medium, are indicative of regional deformities or twists in a liquid film. Periodic waves exhibit recurrent oscillations in a steady, regular pattern over time. Like a curve with a bell, the bell-shaped wave might show lone events or irregularities that affect the liquid film's behaviour. Understanding these wave dynamics in liquid layers is crucial for surface science, material engineering, and fluid mechanics applications. Periodic waves in a liquid film show regular fluctuations, kink waveforms show localized deformations, and shock waves might show sudden disruptions or pressure changes. Bell-shaped lone waves might represent anomalies or isolated incidents that have an impact on the plot of the film.

The proposed mEDAM has the advantage of being simple to use, as it does not require iterative processes or linearization. Its ability to provide a larger range of families of propagating wave solutions, particularly soliton solutions in the shapes of four different function types (trigonometric, hyperbolic, rational, and exponential), makes this a valuable and significant feature that enhances comprehension of the fundamental structures in mathematical simulations. Furthermore, by giving specific values to the free variables associated with it, our technique enables the acquisition of outcomes using other techniques in this niche, including the tanh-coth method, F-expansion approach, sub-equation technique, and (G'/G)-expansion approach. As a consequence, our study shows its breadth and comprehensiveness by serving as a generalization of results produced by other methodologies. It is crucial to remember that the approach encounters difficulties when the highest derivative terms do not homogeneously balance with the largest nonlinear component. This poses a challenge to these approaches' basic technique of creating a homogeneous system of nonlinear algebraic equations.

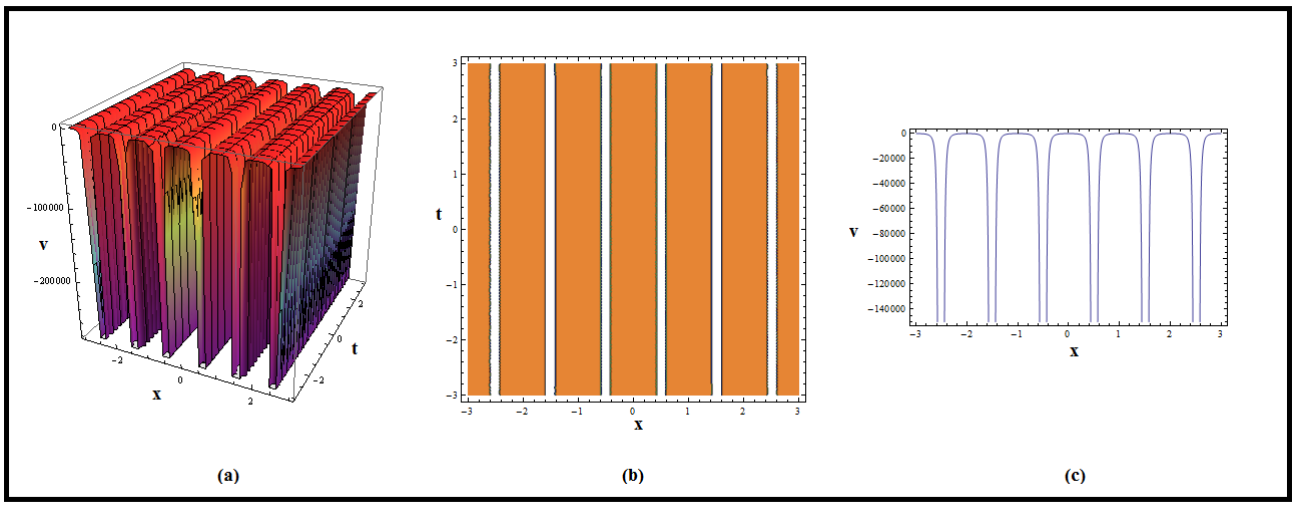

Figure 1. The 3D contour plots of periodic traveling wave $v_{1,1}$ in (3.7) are plotted with $d = 5, e = 1, f = 2, \lambda = 1, \mu = 1$. The 2D graph is constructed simultaneously for $t = 0$. A periodic waveform is a type of wave which recurs frequently throughout time or space.

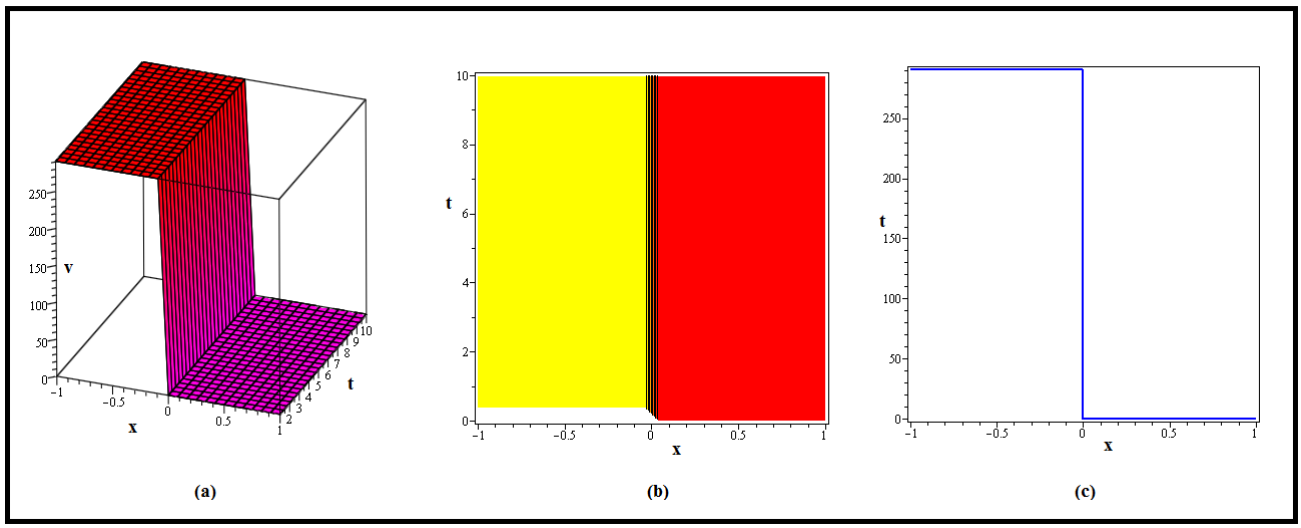

Figure 2. The 3D contour plots of kink traveling wave $v_{1,17}$ in (3.23) are plotted with $d = 3, e = 0, f = -3, \lambda = 0.3, \mu = 0.3$. The 2D graph is constructed simultaneously for $t = 10$. A kink wave is a localized disruption or interruption in a wave's structure that exhibits a sudden shift in amplitude in either direction.

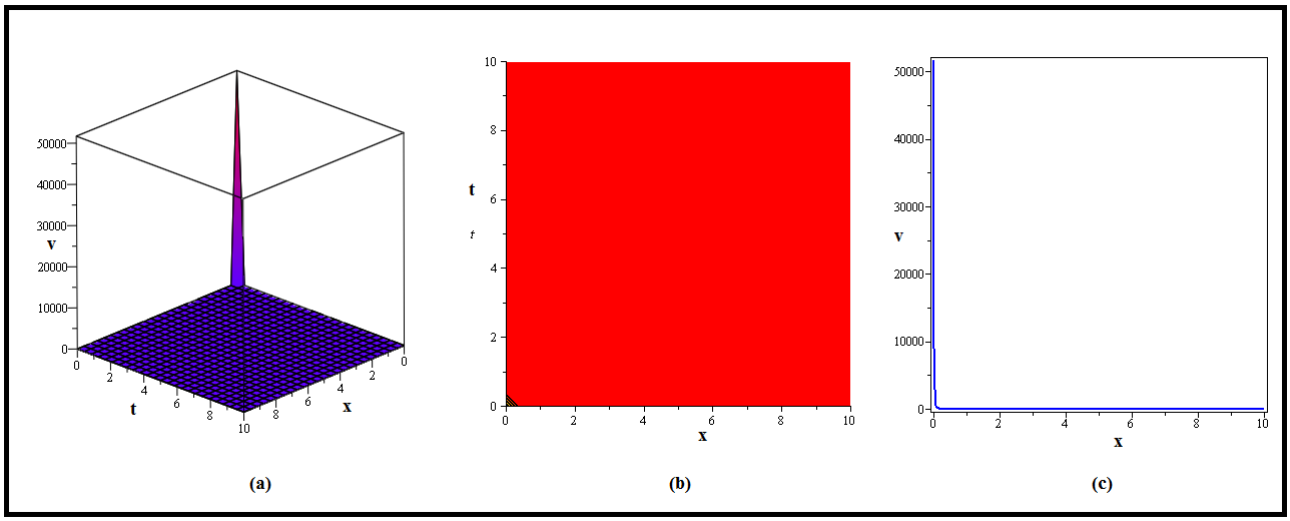

Figure 3. The 3D contour plots of shock traveling wave $v_{1,33}$ in (3.38) are plotted with $d = 0, e = 10, f = 20, s = 2, \kappa = 10, \lambda = 0.9, \mu = 1, p = 1$. The 2D graph is constructed simultaneously for $t = 0$. A shock wave is an abrupt, powerful disruption in a medium that is typified by a sharp rise in density, temperature, and pressure.

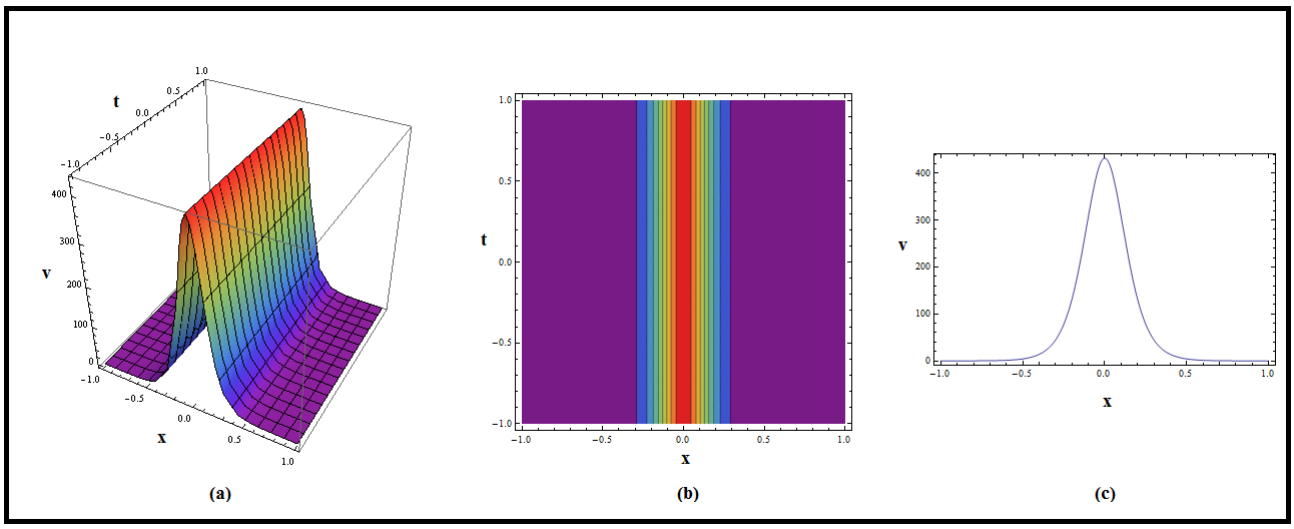

Figure 4. The 3D contour plots of bell-shaped kink traveling wave $v_{2,16}$ in (3.55) are plotted with $d = -3, e = 0, f = 12, \lambda = 1, \mu = 1$. The 2D graph is constructed simultaneously for $t = 0$. A kink waveform with a characteristic bell-shaped pattern that exhibits symmetrical and smooth curve shifts is known as a bell-shaped kink.

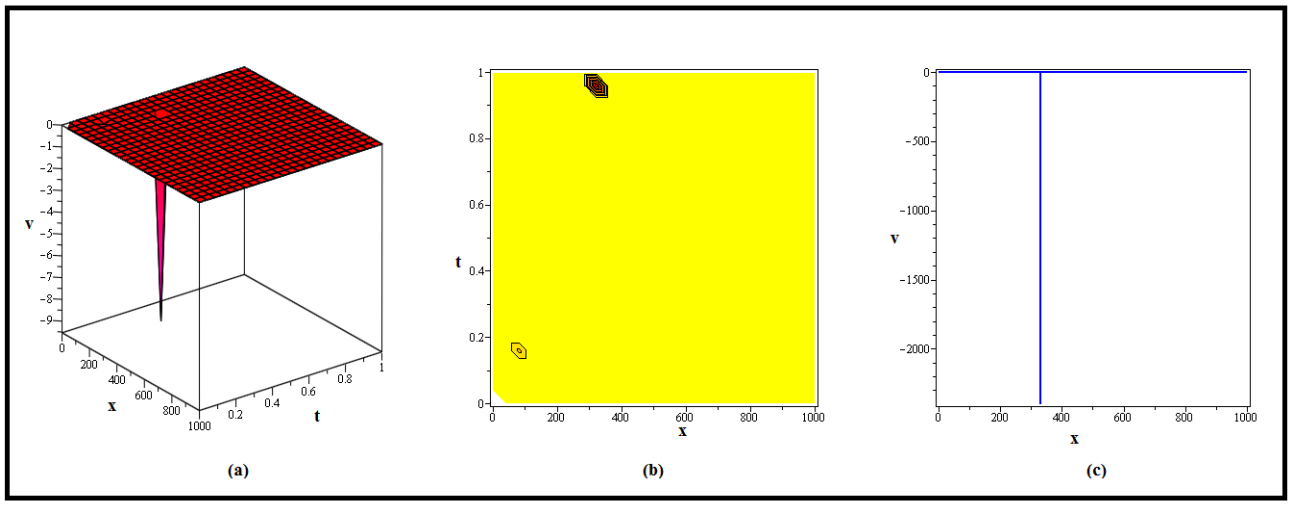

Figure 5. The 3D contour plots of singular kink traveling wave $v_{2,29}$ in (3.68) are plotted with $d = -6, e = 0, f = 6, \lambda = 0.9, \mu = 0.7$. The 2D graph is constructed simultaneously for $t = 1$. A singular kink is a special kind of kink wave that shows non-smooth behavior and extremely high energy concentration at one location.

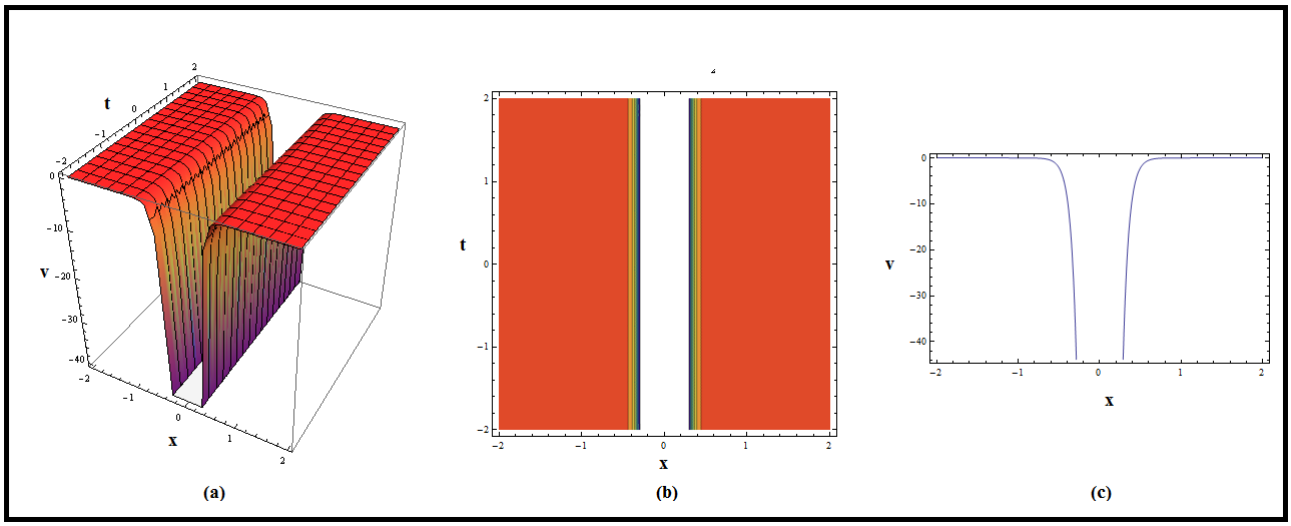

Figure 6. The 3D contour plots of double shock traveling wave $v_{2,30}$ in (3.69) are plotted with $d = -7, e = 0, f = 7, \lambda = 1, \mu = 0.7$. The 2D graph is constructed simultaneously for $t = 0$. A double shock is a profile of two separate shock waves traveling across a medium in an intricate wave structure.

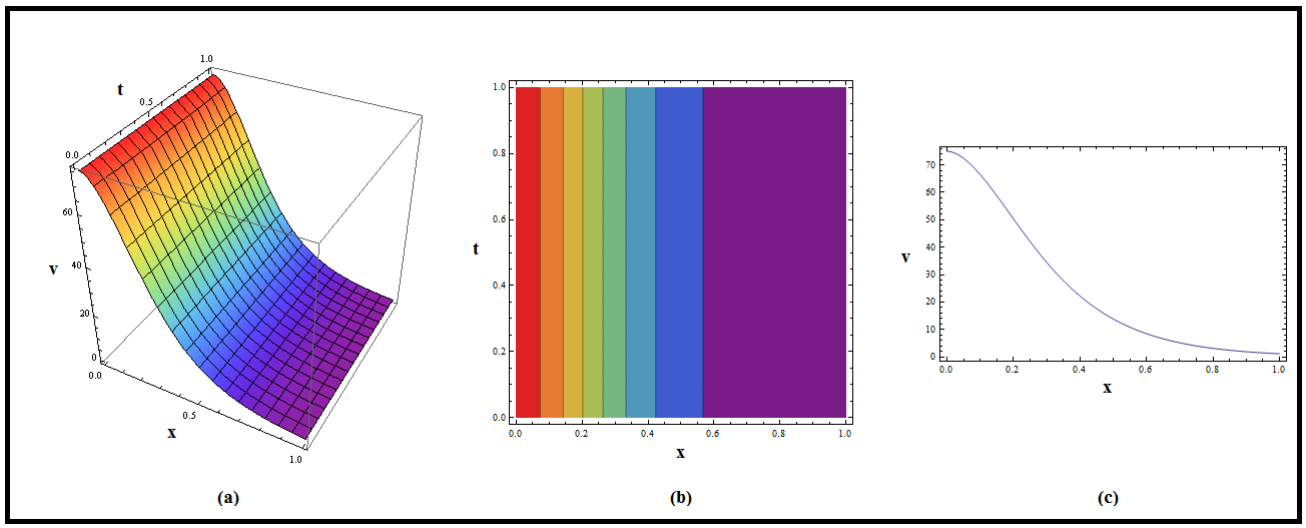

Figure 7. The 3D contour plots of kink traveling wave $v_{2,33}$ in (3.72) are plotted with $d = 0, e = 5, f = 8, \lambda = 0.9, \mu = 0.7$. The 2D graph is constructed simultaneously for $t = 0$. A localized rupture or break in the wave's structure that shows an abrupt change in amplitude in either direction is called a kink wave.

5. Conclusions

In the present research, the propagating wave solutions' families for the CBLE have been developed using the strategic mEDAM. By producing a greater variety of traveling wave solutions in the form of rational, exponential, hyperbolic, and trigonometric functions, which offer a more comprehensive comprehension of the system's underlying dynamics, the proposed approach proved to be beneficial

for nonlinear FPDEs. The traveling wave solutions, comprising periodic, kink, bell-shaped, and shock solitary waves, provided us with vital new information regarding the dynamics of the CBLE. We are able to comprehend these traveling wave solutions and the related wave occurrences more fully due to contour plots and 2D and 3D graphic representations. Overall, this work highlights the need for additional research and real-world applications in a variety of domains, particularly fluid media and plasma physics. It is important to keep in mind that the method becomes problematic if the biggest nonlinear component does not balance homogeneously with the highest derivative terms. This puts into question the fundamental method of these techniques, which is to generate a homogeneous set of nonlinear algebraic equations.

Use of AI tools declaration

The authors declare that they have not used artificial intelligence tools in the creation of this article.

Acknowledgements

The authors extend their appreciation to the Deputyship for Research Innovation, Ministry of Education in Saudi Arabia for funding this research work through the project number ISP-2024.

Conflict of interest

The authors declare that they have no competing interests.

References

1. D. G. Prakasha, P. Veeresha, H. M. Baskonus, Two novel computational techniques for fractional Gardner and Cahn-Hilliard equations, *Comput. Math. Methods*, **1** (2019), e1021.
2. B. Bonilla, M. Rivero, L. Rodriguez-Germa, J. J. Trujillo, Fractional differential equations as alternative models to nonlinear differential equations, *Appl. Math. Comput.*, **187** (2007), 79–88.
3. P. Veeresha, D. G. Prakasha, Solution for fractional generalized Zakharov equations with Mittag-Leffler function, *Results Eng.*, **5** (2020), 100085.
4. J. Liouville, Memoire sur quelques questions de geometrie et de mecanique et sur un nouveau genre de calcul pour rsoudre ces quations, *Ecole Polytech.*, **13** (1832), 71–162.
5. M. Caputo, *Elasticita e dissipazione*, Bologna: Zanichelli, 1969.
6. S. Meng, F. Meng, F. Zhang, Q. Li, Y. Zhang, A. Zemouche, Observer design method for nonlinear generalized systems with nonlinear algebraic constraints with applications, *Automatica*, **162** (2024), 111512. https://doi.org/10.1016/j.automatica.2024.111512
7. B. Li, T. Guan, L. Dai, G. Duan, Distributionally Robust Model Predictive Control with Output Feedback, *IEEE Trans. Autom. Control*, 2023. http://doi.org/10.1109/TAC.2023.3321375
8. Y. Shi, C. Song, Y. Chen, H. Rao, T. Yang, Complex Standard Eigenvalue Problem Derivative Computation for Laminar-Turbulent Transition Prediction, *AIAA J.*, **61** (2023), 3404–3418. http://doi.org/10.2514/1.J062212

9. H. M. He, J. G. Peng, H. Y. Li, Iterative approximation of fixed point problems and variational inequality problems on Hadamard manifolds, *UPB Bull. Ser. A*, **84** (2022), 25–36.
10. R. Subashini, C. Ravichandran, K. Jothimani, H. M. Baskonus, Existence results of Hilfer integro-differential equations with fractional order, *Discrete Contin. Dyn. Syst.-Ser. S*, **13** (2020), 911–923.
11. M. Alqhtani, K. M. Saad, R. Shah, W. M. Hamanah, Discovering novel soliton solutions for (3+1)-modified fractional Zakharov-Kuznetsov equation in electrical engineering through an analytical approach, *Opt. Quant. Electron.*, **55** (2023), 1149.
12. C. Ravichandran, K. Jothimani, H. M. Baskonus, N. Valliammal, New results on nondensely characterized integrodifferential equations with fractional order, *Eur. Phys. J. Plus*, **133** (2018), 109.
13. N. Valliammal, C. Ravichandran, Z. Hammouch, H. Mehmet Baskonus, A new investigation on fractional-ordered neutral differential systems with state-dependent delay, *Int. J. Nonlinear Sci. Numer. Simul.*, **20** (2019), 803–809.
14. S. Noor, A. S. Alshehry, N. H. Aljahdaly, H. M. Dutt, I. Khan, R. Shah, Investigating the impact of fractional non-linearity in the Klein-Fock-Gordon equation on quantum dynamics, *Symmetry*, **15** (2023), 881.
15. T. Abdeljawad, Q. M. Al-Mdallal, F. Jarad, Fractional logistic models in the frame of fractional operators generated by conformable derivatives, *Chaos, Solitons Fractals*, **119** (2019), 94–101.
16. C. Cattani, Connection coefficients of Shannon wavelets, *Math. Modell. Anal.*, **11** (2006), 117–132.
17. A. Jajarmi, B. Ghanbari, D. Baleanu, A new and efficient numerical method for the fractional modeling and optimal control of diabetes and tuberculosis co-existence, *Chaos: Interdiscip. J. Nonlinear Sci.*, **29** (2019), 093111.
18. M. Caputo, M. Fabrizio, On the singular kernels for fractional derivatives. Some applications to partial differential equations, *Progr. Fract. Differ. Appl.*, **7** (2021), 79–82.
19. X. Cai, R. Tang, H. Zhou, Q. Li, S. Ma, D. Wang, et al., Dynamically controlling terahertz wavefronts with cascaded metasurfaces, *Adv. Photonics*, **3** (2021), 036003. http://doi.org/10.1117/1.AP.3.3.036003
20. C. Guo, J. Hu, Y. Wu, S. Celikovsky, Non-Singular Fixed-Time Tracking Control of Uncertain Nonlinear Pure-Feedback Systems With Practical State Constraints, *IEEE Trans. Circuits Syst. I*, **70** (2023), 3746–3758. http://doi.org/10.1109/TCSI.2023.3291700
21. C. Guo, J. Hu, J. Hao, S. Celikovsky, X. Hu, Fixed-time safe tracking control of uncertain high-order nonlinear pure-feedback systems via unified transformation functions, *Kybernetika*, **59** (2023), 342–364. http://doi.org/10.14736/kyb-2023-3-0342
22. X. Bai, Y. He, M. Xu, Low-Thrust Reconfiguration Strategy and Optimization for Formation Flying Using Jordan Normal Form, *IEEE Trans. Aerosp. Electron. Syst.*, **57** (2021), 3279–3295. http://doi.org/10.1109/TAES.2021.3074204
23. Y. Kai, J. Ji, Z. Yin, Study of the generalization of regularized long-wave equation, *Nonlinear Dyn.*, **107** (2022), 2745–2752. http://doi.org/10.1007/s11071-021-07115-6
24. Y. Kai, Z. Yin, On the Gaussian traveling wave solution to a special kind of Schrodinger equation with logarithmic nonlinearity, *Mod. Phys. Lett. B*, **36** (2021), 2150543. http://doi.org/10.1142/S0217984921505436

25. X. Zhou, X. Liu, G. Zhang, L. Jia, X. Wang, Z. Zhao, An Iterative Threshold Algorithm of Log-Sum Regularization for Sparse Problem, *IEEE Trans. Circuits Syst. Video Technol.*, **33** (2023), 4728–4740. http://doi.org/10.1109/TCSVT.2023.3247944
26. D. Benney, Long waves on liquid films, *J. Math. Phys.*, **45** (1966), 150–155.
27. S. P. Lin, Finite amplitude side-band stability of a viscous film, *J. Fluid Mech.*, **63** (1974), 417–429.
28. W. Gao, P. Veeresha, D. G. Prakasha, H. M. Baskonus, New numerical simulation for fractional Benney-Lin equation arising in falling film problems using two novel techniques, *Numer. Methods Partial Differ. Eq.*, **37** (2021), 210–243.
29. N. G. Berloff, L. N. Howard, Solitary and periodic solutions of nonlinear nonintegrable equations, *Stud. Appl. Math.*, **99** (1997), 1–24.
30. H. A. Biagioni, F. Linares, On the Benney–Lin and Kawahara equations, *J. Math. Anal. Appl.*, **211** (1997), 131–152.
31. S. B. Cui, D. G. Deng, S. P. Tao, Global existence of solutions for the Cauchy problem of the Kawahara equation with L 2 initial data, *Acta Math. Sin.*, **22** (2006), 1457–1466.
32. H. Tariq, G. Akram, Residual power series method for solving time-space-fractional Benney-Lin equation arising in falling film problems, *J. Appl. Math. Comput.*, **55** (2017), 683–708.
33. P. K. Gupta, Approximate analytical solutions of fractional Benney–Lin equation by reduced differential transform method and the homotopy perturbation method, *Comput. Math. Appl.*, **61** (2011), 2829–2842.
34. Y. X. Xie, New explicit and exact solutions of the Benney-Kawahara-Lin equation, *Chin. Phys. B*, **18** (2009), 4094.
35. K. K. Ali, R. Yilmazer, H. M. Baskonus, H. Bulut, Modulation instability analysis and analytical solutions to the system of equations for the ion sound and Langmuir waves, *Phys. Scr.*, **95** (2020), 065602.
36. H. Qin, R. A. Attia, M. Khater, D. Lu, Ample soliton waves for the crystal lattice formation of the conformable time-fractional (N+ 1) Sinh-Gordon equation by the modified Khater method and the Painleve property, *J. Intell. Fuzzy Syst.*, **38** (2020), 2745–2752.
37. A. Gaber, H. Ahmad, Solitary wave solutions for space-time fractional coupled integrable dispersionless system via generalized kudryashov method, *Facta Univ. Ser.: Math. Inf.*, **35** (2021), 1439–1449.
38. H. Yasmin, A. S. Alshehry, A. M. Saeed, R. Shah, K. Nonlaopon, Application of the q-Homotopy Analysis Transform Method to Fractional-Order Kolmogorov and Rosenau-Hyman Models within the Atangana-Baleanu Operator, *Symmetry*, **15** (2023), 671.
39. J. H. He, Exp-function method for fractional differential equations, *Int. J. Nonlinear Sci. Numer. Simul.*, **14** (2013), 363–366.
40. H. Khan, R. Shah, J. F. Goómez-Aguilar, D. Baleanu, P. Kumam, Traveling waves solution for fractional-order biological population model, *Math. Modell. Nat. Phenom.*, **16** (2021), 32.
41. H. Yasmin, N. H. Aljahdaly, A. M. Saeed, R. Shah, Investigating Symmetric Soliton Solutions for the Fractional Coupled Konno-Onno System Using Improved Versions of a Novel Analytical Technique, *Mathematics*, **11** (2023), 2686.
42. M. M. Al-Sawalha, H. Yasmin, R. Shah, A. H. Ganie, K. Moaddy, Unraveling the Dynamics of Singular Stochastic Solitons in Stochastic Fractional Kuramoto–Sivashinsky Equation, *Fractal Fract.*, **7** (2023), 753.

43. M. Alquran, Dynamic behavior of explicit elliptic and quasi periodic-wave solutions to the generalized (2+ 1)-dimensional Kundu-Mukherjee-Naskar equation, *Optik*, **301** (2024), 171697.
44. H. Yasmin, A. S. Alshehry, A. H. Ganie, A. M. Mahnashi, Perturbed Gerdjikov-Ivanov equation: Soliton solutions via Backlund transformation, *Optik*, **298** (2024), 171576.
45. I. Jaradat, M. Alquran, A variety of physical structures to the generalized equal-width equation derived from Wazwaz-Benjamin-Bona-Mahony model, *J. Ocean Eng. Sci.*, **7** (2022), 244–247.
46. S. A. El-Tantawy, H. A. Alyousef, R. T. Matoog, R. Shah, On the optical soliton solutions to the fractional complex structured (1+ 1)-dimensional perturbed gerdjikov-ivanov equation, *Phys. Scr.*, **99** (2024), 035249.
47. M. Alquran, Necessary conditions for convex-periodic, elliptic-periodic, inclined-periodic, and rogue wave-solutions to exist for the multi-dispersions Schrodinger equation, *Phys. Scr.*, **99** (2024), 025248.
48. M. Alquran, The amazing fractional Maclaurin series for solving different types of fractional mathematical problems that arise in physics and engineering, *Partial Differ. Eq. Appl. Math.*, **7** (2023), 100506.
49. S. Alshammari, K. Moaddy, M. Alshammari, Z. Alsheekhhussain, M. M. Al-Sawalha, M. Yar, Analysis of solitary wave solutions in the fractional-order Kundu-Eckhaus system, *Sci. Rep.*, **14** (2024), 3688.
50. S. Mukhtar, S. Noor, The numerical investigation of a fractional-order multi-dimensional Model of Navier-Stokes equation via novel techniques, *Symmetry*, **14** (2022), 1102.
51. P. Sunthrayuth, A. M. Zidan, S. W. Yao, M. Inc, The comparative study for solving fractional-order Fornberg-Whitham equation via ρ-Laplace transform, *Symmetry*, **13** (2021), 784.
52. R. Shah, D. Baleanu, Fractional Whitham-Broer-Kaup equations within modified analytical approaches, *Axioms*, **8** (2019), 125.
53. A. Saad Alshehry, M. Imran, A. Khan, W. Weera, Fractional View Analysis of Kuramoto-Sivashinsky Equations with Non-Singular Kernel Operators, *Symmetry*, **14** (2022), 1463.
54. M. M. Al-Sawalha, A. Khan, O. Y. Ababneh, T. Botmart, Fractional view analysis of Kersten-Krasil'shchik coupled KdV-mKdV systems with non-singular kernel derivatives, *AIMS Mathematics*, **7** (2022), 18334–18359. https://doi.org/10.3934/math.20221010
55. H. Yasmin, A. S. Alshehry, A. H. Ganie, A. Shafee, R. Shah, Noise effect on soliton phenomena in fractional stochastic Kraenkel-Manna-Merle system arising in ferromagnetic materials, *Sci. Rep.*, **14** (2024), 1810.
56. J. H. He, S. K. Elagan, Z. B. Li, Geometrical explanation of the fractional complex transform and derivative chain rule for fractional calculus, *Phys. Lett. A*, **376** (2012), 257–259.
57. Sarikaya, M. Zeki, H. Budak, H. Usta, On generalized the conformable fractional calculus, *TWMS J. Appl. Eng. Math.*, **9** (2019), 792–799.